HERSCHEL / PLANCK

Cryostat Shielding Efficiency Assessment Consolidation

Product Code : 10000

Rédigé par/*Written by*	Responsabilité-Service-Société *Responsibility-Office -Company*	Date	Signature
M. NADARASSIN	RF Analysis	28/05/04	
Vérifié par/*Verified by*			
A. LUC	EMC Engineer	28/05/04	
P. RIDEAU	Engineering Manager	02/06/04	
Approbation/*Approved*			
J-J. JUILLET	Project Manager	03/06/04	

Data management : G. SERRA

Entité Emettrice : Alcatel Space - Cannes
(détentrice de l'original) :

HERSCHEL/PLANCK	DISTRIBUTION RECORD		
DOCUMENT NUMBER : H-P-2-ASPI-TN-0177		Issue 2 / Rev. : Date: 28/05/2004	
EXTERNAL DISTRIBUTION		INTERNAL DISTRIBUTION	
ESA	X	HP team	X
ASTRIUM	X		
ALENIA			
CONTRAVES			
TICRA			
TECNOLOGICA			
		Clt Documentation	Orig.

ENREGISTREMENT DES EVOLUTIONS / CHANGE RECORDS

ISSUE	DATE	§ : DESCRIPTION DES EVOLUTIONS § : CHANGE RECORD	REDACTEUR AUTHOR
1	30/11/2001	Initial Issue	L. TROUGNOU
2	27/05/2004	Document completely revised	M. NADARASSIN

TABLE OF CONTENTS

LIST OF FIGURES

LIST OF TABLES

1. INTRODUCTION

1.1 Purpose of this note

This note deals with the electromagnetic coupling between the SVM and the focal plane of the Herschel Telescope. More precisely, any external spurious source of electromagnetic field could have an impact on the instruments placed at the focal plane if its level is high. The SVM is assumed to be a source of spurious field.
To carry out the simulation, the geometry of the spacecraft has been taken into account and a model for an electromagnetic source has been defined.
By performing a MGTD+PO+PTD simulation through GRASP8, the field in the focal plane has been computed and the coupling factor deduced.

The frequencies for the simulations are taken in the 2.4 to 8GHz band.

#

1.2 Reference and applicable documents

1.2.1 Applicable documents

[AD1]	H-P-1-ASPI-SP-0037	HERSCHEL/PLANCK EMC Specification
[AD2]	H-P-1-ASPI-PL-0038	HERSCHEL/PLANCK EMC/ESD Control Plan
[AD3]	SCI-PT-IIDB/HIFI-02125	‘HIFI’ Instrument Interface Document – Part B

1.2.2 Reference documents

[RD1]	GRASP8 Software (TICRA)	Technical Description, TICRA Engineering Consultants.

1.3 Acronyms

HP	Herschel-Planck
SRS	System Requirements Specification
MGTD	Multi geometry theory of diffraction
PO	Physical optics
PTD	Physical theory of diffraction

2. ANALYSIS

2.1 Herschel specification and source definition

The specification for Herschel is illustrated in the Figure 2.1 below.

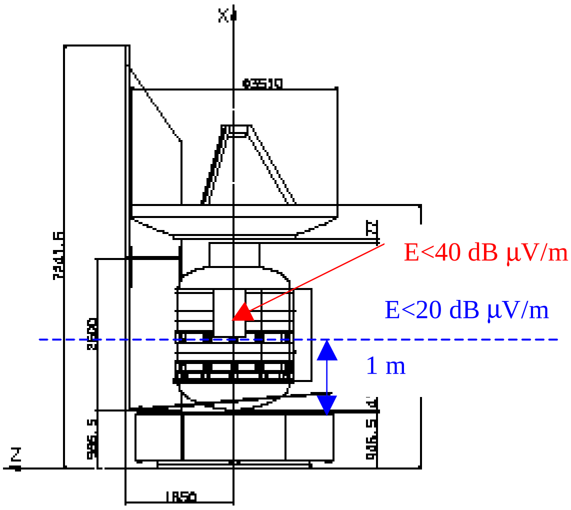

Figure 2-1 Hershel specifications

Herschel spacecraft is concerned by two specifications in term of maximum value of E-field (Figure 2-1) :

1) the E-field measured at a distance of 1 m from the SVM upper surface must be lower than 20 dBµV/m (Ref. AD1)

2) the E-field amplitude in the tank must be lower than 40 dBµV/m (Ref. AD3)

The method proposed in this study to simulate the coupling is to replace the SVM by a source of electromagnetic field and verifying the specification 1 (E<20 dB µV/m at 1 meter from the SVM) and then compute the field at the focal plane.
The field distribution on the SVM is not known, only the level is specified. As long as there are no assumption on it, the simplest way is to consider an incident plane wave propagating from the SVM to the telescope. The plane wave having the same magnitude at any point of the plane. Consequently, this source is a worst case situation. The amplitude of the field created by this plane wave will be scaled to obtain the specification in term of E field at 1 meter from the SVM (see § 2.2.3).

2.2 Grasp8 model

2.2.1 Geometry and ray paths

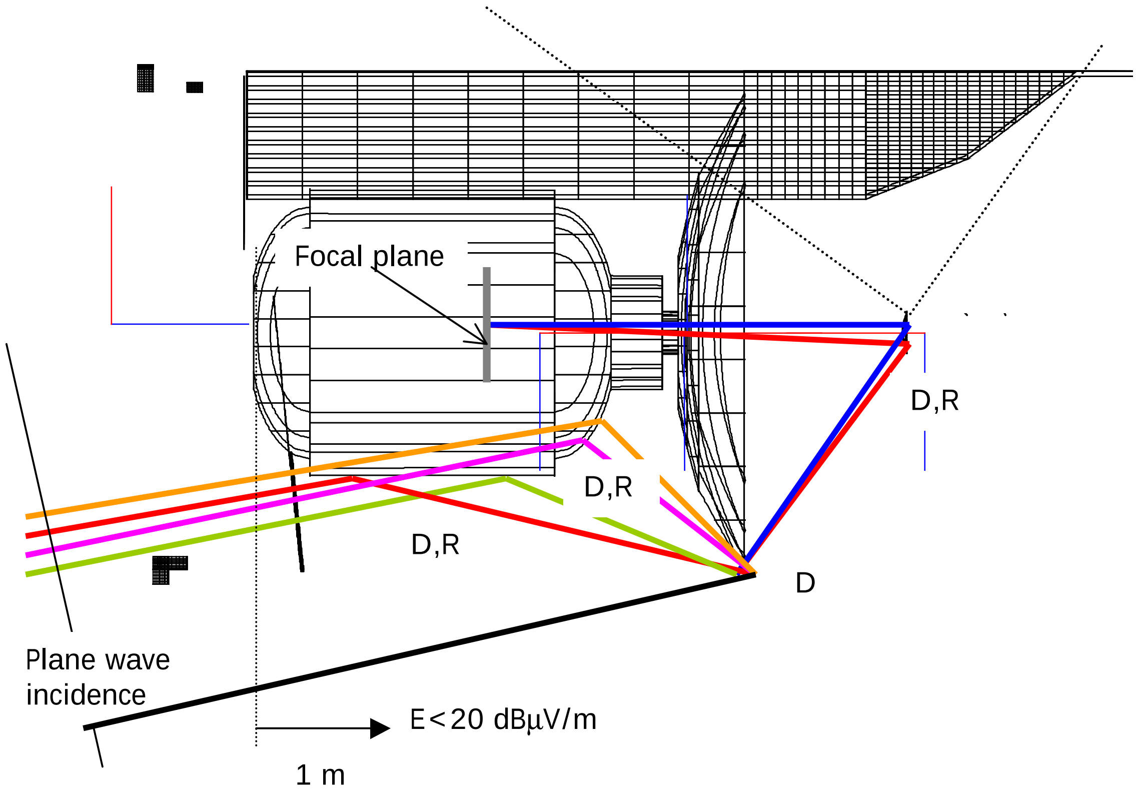

Figure 2-2 GRASP 8 model : different paths for the GTD computation

The field propagating from the SVM encounters different blockages which can modify significantly the way it propagates before reaching the focal plane. Nevertheless, a simplified model of Herschel must be taken in order to reduce the computation effort. Thus, the elements which do not have a significant impact have been removed from the model.

Figure 2.2 shows the geometrical model used for the computation, preliminary computation allowed to select the main contributors. In Figure 2.3 is plotted the far field of the telescope in the main optical axis, the method used is the MGTD performed with Grasp8 module . The feed is placed at the focal point of the telescope, the frequency of the simulation is 30GHz. The diffraction at the angle of 127° is the diffraction of the field at the edge of the main reflector. As a consequence, an electromagnetic field which diffracts at the edge of the main reflector could reach the focal plane. Thus, the field coming from the SVM and diffracting at the edge of the main reflector is the major contributor. This last remark is taken into account for the simulation. Concerning the blockage at the angle –140 degrees and at –55 degrees, this is due to the solar panel. One can compute the diffraction at these angles. Due to the geometry of the structure the field are reflected from the solar panel in a direction of <-90 degrees. The diffraction at the upper edge of the solar panel gives a maximum around -55 degrees. In our case the source of spurious field come from the backside of the telescope with a propagation angle –180 degrees. The only realistic way for an electromagnetic field to reach the telescope focal plane is the diffraction at the edge of the main reflector and follow the focusing way of the telescope (main-reflector- sub-reflector-focal point) . The other paths (main-reflector- solar panel -focal point) or (main-reflector- solar panel –sub-reflector focal point) are negligible or of third order.

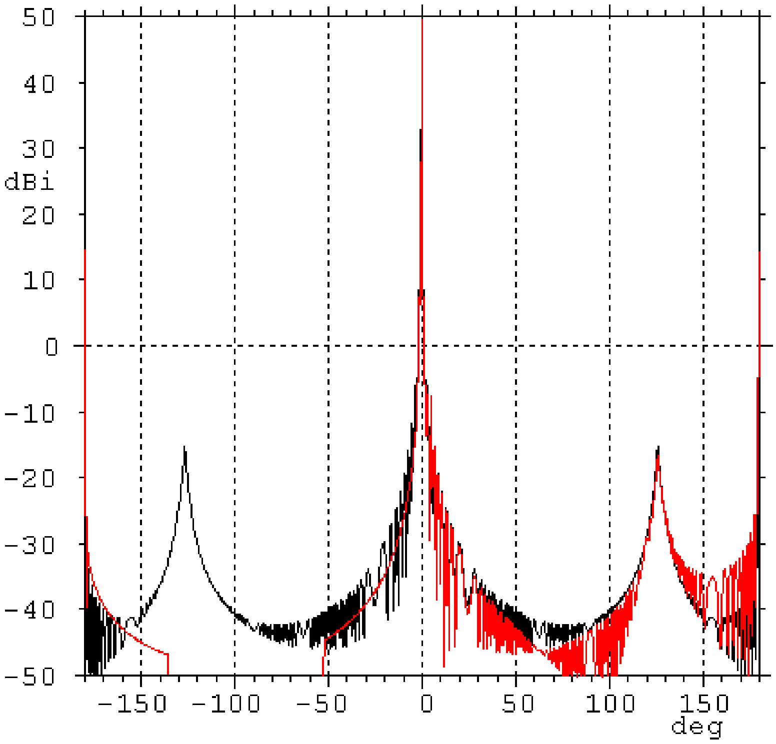

Figure 2-3 Far field pattern of the telescope. Feed at 30GHz (black : without blockage solar panel, and grey with blockage)

We have noticed that the diffraction on the main reflector is the major contributor. Consequently, to be consistent, all the second and third order paths passing finally by a diffraction on the main reflector have to be considered.

This concerns the reflection and the diffraction of the field generated at SVM level by the solar panel and the tank.

The tank is composed by 3 parts :

Tank1 : inferior part
Tank2 : main part
Tank3 : superior part

The solar panel is composed of several parts. As noticed in the previous chapter, its impact is negligible. The paths reflecting or diffracting by this way could not reach the focal plane.

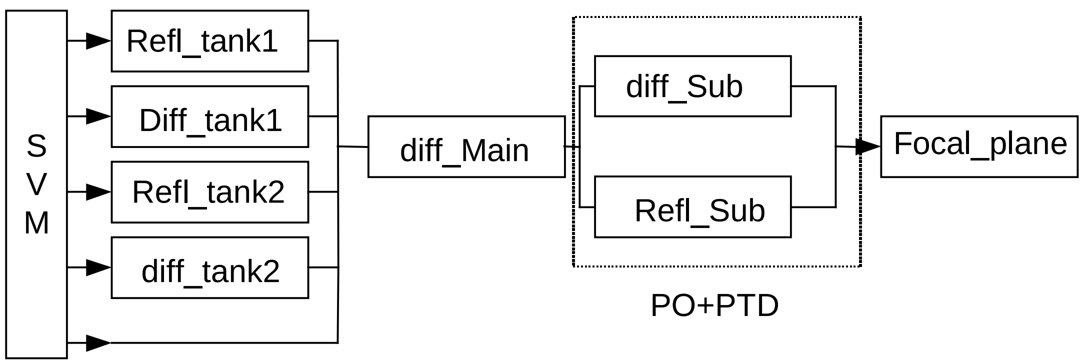

Figure 2-4 Coupling between SVM and Focal plane

Concerning the tank see Figure 2-4 above, the diffraction and reflection have been considered.

2.2.2 Method of simulation

Figure 2-4 provides a description of the many contributors to the field in the focal plane. The field is calculated in a planar grid of dimension 1m*1 m placed at the focus of the telescope. The different paths identified as likely to have an impact are the direct path (SVM diffration by the main diffraction, reflection by the sub) and the others which before reaching the main reflector diffract or reflect on the tank. The lower part of the tank is not considered because its impact is negligible due to the blockage of the middle part of the tank.

The method which is generally used to simulate the electromagnetic field in such an environment is the MGTD (multi-GTD). Faster than full PO , the MGTD is currently employed for large object with some limitations. Due to caustics problems, the computation of the field at an angle near the RF axis is erroneous. In our case full MGTD could not be applied. That is why, for the computation of the field near the RF axis, the PO+PTD is used.
The E-Field level has been computed using MGTD and PO+PTD by considering the main paths. In other words only the scatterers wich induce a non neglectable E_field in the focal plane have been taken into account in the final GTD PO+PTD computation.

2.2.3 Field normalization

We use a plane wave as a source of excitation in the Grasp8 model. The plane wave in Grap8 is defined by an aperture radius. The plane wave is defined as containing $P=4\pi$ power in a disk of radius of curvature R which means :

$$P = 4\pi = \int_S E \wedge H \, ds = \frac{1}{2}\frac{E^2 \pi R^2}{Z_0} \qquad (1)$$

with Z_0 the vacuum impedance.
The electric field is given by:

$$E = \sqrt{\frac{8Z_0}{R^2}} \qquad (2)$$

Grasp8 gives a normalized field which is proportionnal to the real field :

$$E = k\sqrt{2Z_0}E_{grasp} \qquad (3)$$

then the value of the field given by Grasp8 is :

$$E_{grasp_{dB}} = 20\log_{10}\left(\frac{2}{kR}\right) \qquad (4)$$

We want a field of 20 dB µV/m propagating from the SVM . To obtain this value we have to choose a value of R verifying equation (2). This gives R=5462534.34 m. An other way is to consider a fixed radius of curvature for example R_x and then subtract to the computed field the log of the ratio:

$$E_{grasp_{dB}}(R) = E_{grasp_{dB}}(R_x) - 20\log_{10}(R/R_x) \qquad (5)$$

In our analysis the aperture radius is fixed to 4 m because the SVM has a limited surface. To obtain the electric field of 20 dB µV/m , we subtract 122.7 dB from the results.

3. SIMULATION RESULTS

3.1 Main contributors

2 curves are represented in Figure 3.1 :

Field computed with

path : dm_ PO+PTD

Field computed with all theses paths :

path : dm_ PO+PTD
path : d1_dm_ PO+PTD
path : r2_dm_ PO+PTD
path : d2_dm_ PO+PTD
path : r1_dm_ PO+PTD
path : d1_dm_ PO+PTD
path : r2_dm_ PO+PTD
path : d2_dm_ PO+PTD

As we could expect, the major contibutors are the two second order paths dm_ PO+PTD. The other paths contribute only for a minor part.

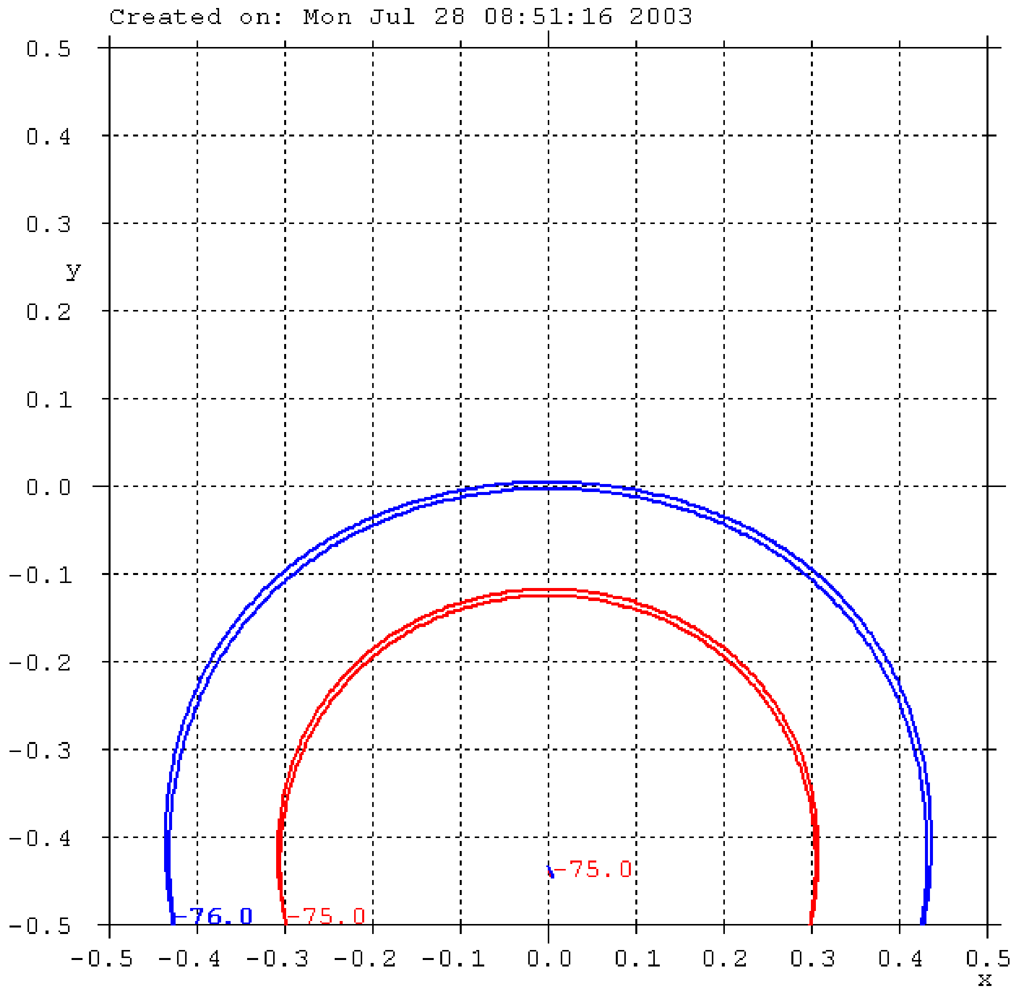

Figure 3-1 2.4 GHz : Total field dm_PO+PTD and total contribution (Peak –73.96 dB and –73.99 dB)

3.2 Impact of plane wave incidence angle

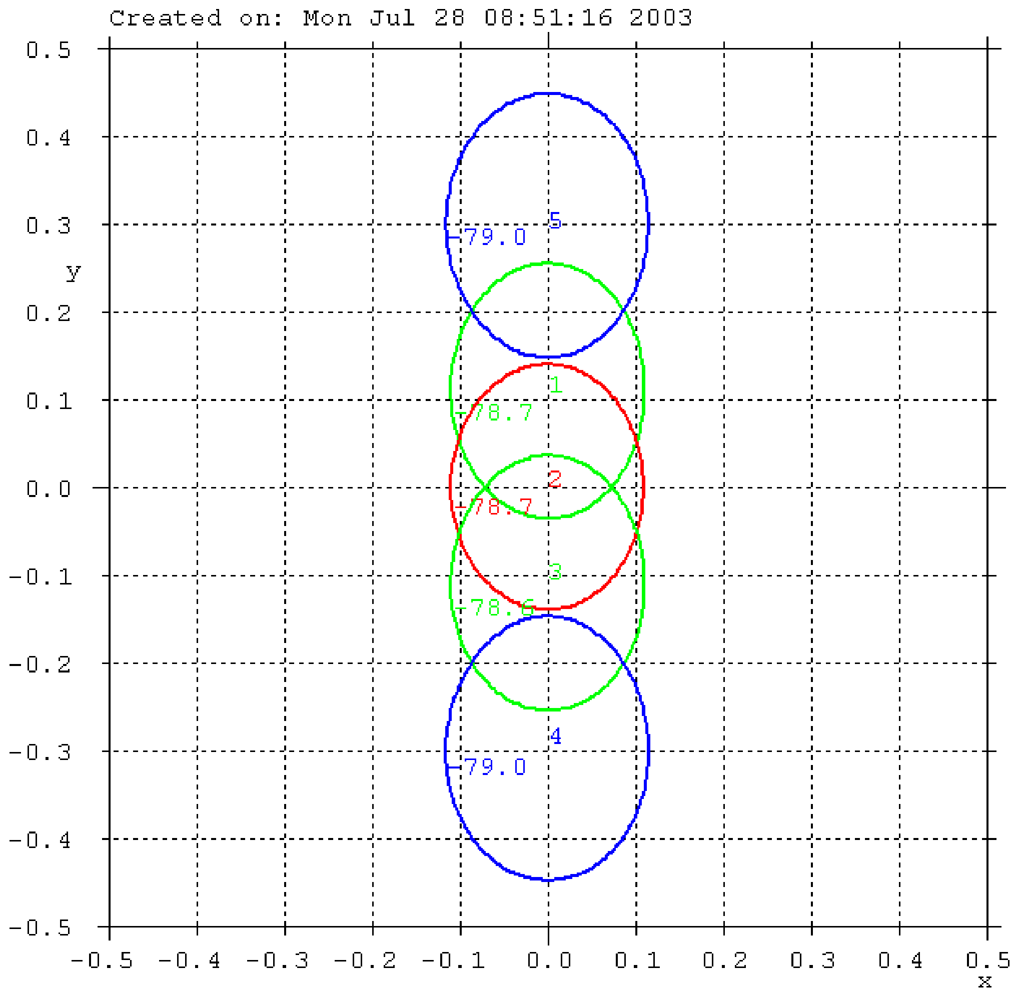

Figure 3-2 Impact of incidence angle –0.5, -0.2, 0, 0.2, 0.5 degrees, Contour level –1 dB

In Figure 3-2, the field in the focal plane is plotted for different plane wave incidences. As we could expect, a displacement of the focusing point in the plane of the angular incidence variation is observed. If we look at the figure 3-2, the rays coming from the sub reflector pass through the main reflector center hole and the telescope baffle which block one part of the rays. The center hole diameter is 560 mm and the telescope baffle diameter is 246 mm. The rays are blocked by the main reflector beyond an incidence angle of 3.5 degrees. As a consequence, there is no electric field beyond a diameter of 600 mm in the focal plane. Then a plane wave with an incidence angle superior to 0.5 degrees are blocked and could not reach the focal plane.

Incidence angle	E grasp
degrees	dB
-0,5	-78,03
-0,2	-77,65
0	-77,71
0,2	-77,63
0,5	-78,01

Table 3-1 E variation versus incidence angle (maximum)

3.3 Field intensity versus frequency

In Figure 3.3 , the fields in the focal plane are plotted for different frequencies (2.4 GHz, 3.8 GHz, 5.2 GHz, 6.6 GHz, 8 GHz) The field intensity decreases with frequencies. In Table 3.2 , the numerical values of the maximum are given (E field grasp8 normalized values).

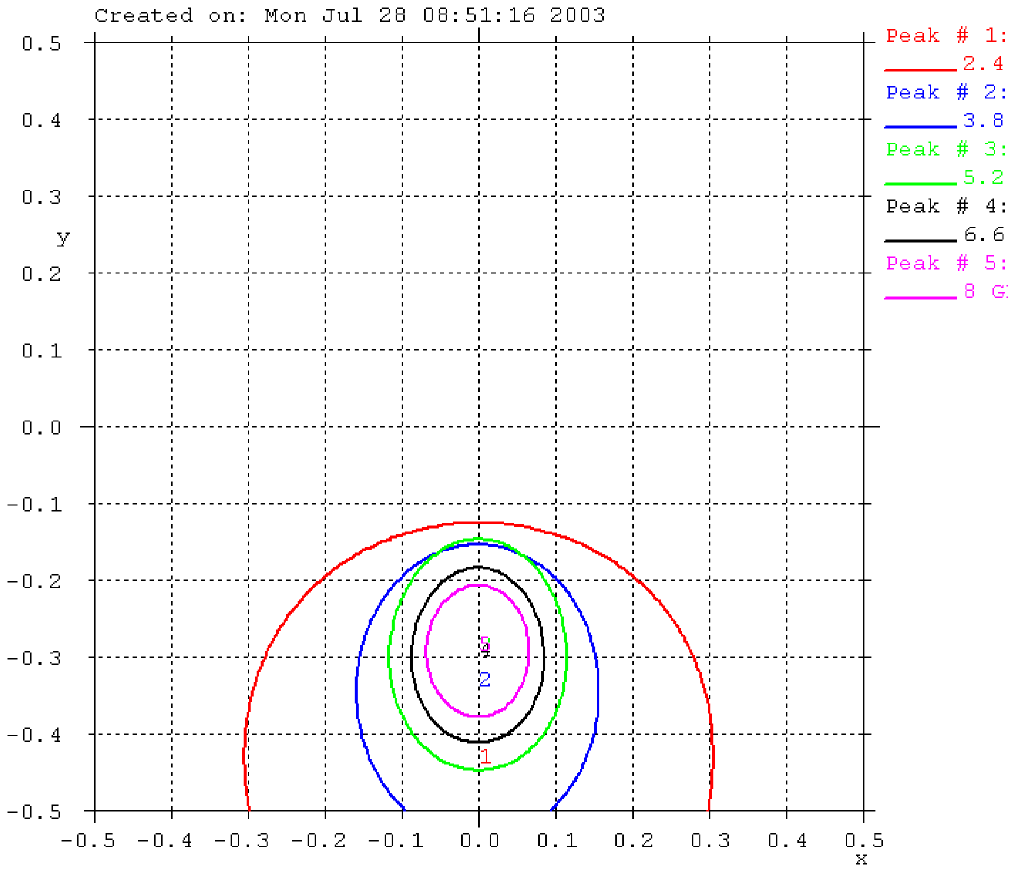

Figure 3-3 Fields in the focal plane (2.4 GHz , 3.8 GHz, 5.2 GHz, 6.6 GHz, 8 GHz). Contour level –1 dB. Incidence angle 0.5 degrees.

Frequency GHz	Peak Egrasp dB
2,4	-73,96
3,8	-77,03
5,2	-78,01
6,6	-81,18
8	-83,47

Table 3-2 Max level of the field in the focal plane versus frequency

Table 3.3 gives the values of the E-field on the focal plane.

AT THE FOCAL PLANE

normalisation dB	E(dB grasp) dB (grasp)	E(DB grasp) corrected dB (grasp)	E grasp	Frequency GHz	l m	k m-1	Zo W	E (focal plane) V/m	E dB mV/m	decoupling E_svm/E_focal	decoupling dB
-122,7	-69,14	-191,84	2,55859E-10	2	0,1500	41,89	376,98	2,94E-07	-10,63	33,98	30,6
-122,7	-73,96	-196,66	1,46893E-10	2,4	0,1250	50,26	376,98	2,03E-07	-13,86	49,33	33,9
-122,7	-77,03	-199,73	1,03157E-10	3,8	0,0789	79,58	376,98	2,25E-07	-12,94	44,36	32,9
-122,7	-78,01	-200,71	9,2151E-11	5,2	0,0577	108,91	376,98	2,76E-07	-11,20	36,29	31,2
-122,7	-81,18	-203,88	6,39735E-11	6,6	0,0455	138,23	376,98	2,43E-07	-12,29	41,18	32,3
-122,7	-82,56	-205,26	5,45758E-11	7,4	0,0405	154,98	376,98	2,32E-07	-12,68	43,06	32,7
-122,7	-83,48	-206,18	4,90908E-11	8	0,0375	167,55	376,98	2,26E-07	-12,92	44,28	32,9
-122,7	-83,7	-206,4	4,7863E-11	10	0,0300	209,43	376,98	2,75E-07	-11,21	36,33	31,2
-122,7	-87,66	-210,36	3,03389E-11	15	0,0200	314,15	376,98	2,62E-07	-11,64	38,21	31,6
-122,7	-90,89	-213,59	2,0917E-11	20	0,0150	418,87	376,98	2,41E-07	-12,38	41,57	32,4

Table 3-3 Decoupling between the SVM plane and the focal plane.

The decoupling factor is around 30dB. The strength of the E-field in the tank cavity remains small compared to field generated by the SVM.

4. CONCLUSION

In this note, the analysis of the decoupling between the SVM and the focal plane of Herschel is proposed. By considering a worst case situation for source of spurious field generated by the SVM, the field inside the tank is computed by MGTD and PO+PTD analysis by using Grasp8 module.

As a conclusion, the magnitudes of the computed fields remain small compared to the specified values. Due to numerous blockage and imperfect edge surface, the field really expected must be lower than the calculated values which provides us with a comfortable margin.

The analysis indicates a decoupling factor of greater than 30dB between the Focal Plane and the maximum allowable E-field generated at the SVM.

END OF DOCUMENT